Neural network model reference decoupling control for single leg joint of hydraulic quadruped robot

Bingwei Gao
College of Mechanical and Power Engineering, Harbin University of Science and Technology, Harbin, China, and
Wenlong Han
Power Station Equipment Filiale Harbin Fenghua Co., Ltd, Harbin, China and Aerospace Science and Industry Corp., Harbin, China

Abstract

Purpose – To control one of the joints during the actual movement of the hydraulically driven quadruped robot, all the other joints in the leg need to be locked. Once the joints are unlocked, there is a coupling effect among the joints. Therefore, during the normal exercise of the robot, the movement of each joint is affected by the coupling of other joints. This brings great difficulties to the coordinated motion control of the multi-joints of the robot. Therefore, it is necessary to reduce the influence of the coupling of the hydraulically driven quadruped robot.

Design/methodology/approach – To solve the coupling problem with the joints of the hydraulic quadruped robot, based on the principle of mechanism dynamics and hydraulic control, the dynamic mathematical model of the single leg mechanism of the hydraulic quadruped robot is established. On this basis, the coupling dynamics model of the two joints of the thigh and the calf is derived. On the basis of the multivariable decoupling theory, a neural network (NN) model reference decoupling controller is designed.

Findings – The simulation and prototype experiment are carried out between the thigh joint and the calf joint of the hydraulic quadruped robot, and the results show that the proposed NN model reference decoupling control method is effective, and this method can reduce the cross-coupling between the thigh and the calf and improve the dynamic characteristics of the single joint of the leg.

Practical implications – The proposed method provides technical support for the mechanical–hydraulic cross-coupling among the joints of the hydraulic quadruped robot, achieving coordinated movement of multiple joints of the robot and promoting the performance and automation level of the hydraulic quadruped robot.

Originality/value – On the basis of the theory of multivariable decoupling, a new decoupling control method is proposed, in which the mechanical–hydraulic coupling is taken as the coupling behavior of the hydraulic foot robot. The method reduces the influence of coupling of system, improves the control precision, realizes the coordinated movement among multiple joints and promotes the popularization and use of the hydraulically driven quadruped robot.

Keywords Neural network, Control method, Joint decoupling, Model reference, Quadruped robot

Paper type Research paper

1. Introduction

The hydraulic quadruped robot is a highly complex nonlinear and strong coupling system with multi inputs and multi outputs. In general, the output of other joint will affect the input of one joint, and at the same time, the output of the joint also affects the input of the other joint (Ding *et al.*, 2007; Ding and Liu, 2011). Therefore, there is a coupling phenomenon among the joints. This brings a lot of difficulties to the motion control of the quadruped robot, so the decoupling among the joints of the robot becomes one of the most difficult problems.

For the coupling problem, many control strategies are studied. Kayacan *et al.* (2011) introduced the dynamic modeling and control analysis of the spherical robot. The kinematics of the model was analyzed by the classical method of the rotation matrix. The dynamic modeling of the system was based on Euler–Lagrange form. By means of dynamic decoupling method, the nonholonomic and highly nonlinear equations of motion were decomposed into two simple subsystems, and the dynamic decoupling control was realized. To solve the unbalanced and mechanical coupling problem in the industrial control, Iván *et al.* (2012) established a dynamic model and then completed the simulation, and proposed feedforward decoupling control algorithms. The experimental results showed that this control method improved the performance of the control system compared with the independent axis control method. Nikolaou and Hanagandi (1995) used the synergy between modeling and recurrent neural network (NN); recurrent NN was used conveniently to

The current issue and full text archive of this journal is available on Emerald Insight at: **www.emeraldinsight.com/0144-5154.htm**

Assembly Automation
38/4 (2018) 465–475

[DOI 10.1108/AA-08-2017-098]

Received 3 September 2017
Revised 26 October 2017
4 December 2017
6 January 2018
28 February 2018
Accepted 5 March 2018

integrated black-box modeling and to design the decoupling controller for nonlinear multivariable control system, and the decoupling performance that effects from model uncertainty on the system state reconstruction were discussed. Nicuols (1982) used the Pontryagin maximum principle; the state space control by extra non-difference inequality constrained problems was solved. To solve the control problem of multi-inputs and multi-outputs system, a time optimal decoupling control method was proposed. The performance index function of robust decoupling in the state space was obtained by Wang *et al.* (1994). On the basis of the state feedback, this paper presented a robust decoupling control method with robust stability, and the algorithm was applied to multi-joints of robot's control system driven by the electric hydraumatic, and the simulation and analysis were carried out, which provided reference to the design of decoupling system. The optimization method of modern control theory was applied by Luo *et al.* (1992), and the electrohydraulic servo system of the articulated robot was studied, which proved that it was effective to eliminate the coupling effect among the degrees of freedom and improve the performance of the system. The method of the first kind Lagrange equation was used by Liu *et al.* (2009), and the dynamic model of parallel robot was established. According to the model, the numerical simulation of decoupling control was carried out, and at the same time, an improved decoupling control method was proposed for calculating the torque. Through the analysis of the simulation results, it was proved that the decoupling control method made the robot system achieve high control precision. Lin and Kuroe (1995) proposed a variable-structure disturbance observer and a method for decoupling control of robot manipulators by applying the proposed observer. The proposed observer can treat a general class of disturbances and overcome the problems of the conventional disturbance observers, that is, sensitiveness to sensor noise and delay of convergence. The proposed control method was implemented into an experimental 3-degree-of-freedom DD robot. It was shown through the experimental results that the proposed method could realize decoupling control for robot manipulators more precisely and robustly. Michael and Makoto (2015) proposed and evaluated the feed-forward decoupling of joint torque in elastic joint robots. The joint elasticities, captured by the third-order polynomial function, were considered together with the inverse manipulator dynamics so as to provide the required driving torque for the reference trajectories. Therewith decoupled joint actuators can be robustly controlled in a feedback manner for which a convenient proportional-derivative regulation was sufficient. Using the inverse manipulator dynamics and joint model, the reference value in the joint output (load) and not input (motor) space was provided to the feedback control of decoupled actuators. This allowed compensating for the joint torsion and improved the load positioning accuracy without output sensors. Takahiro *et al.* (2014) extended the diagonalization method on the basis of the modal space disturbance observer (MDOB) for application to a multi-degree-of-freedom (DOF) system. The aim of this method was to suppress the interference between the position and force control systems and realize a bilateral control system. The utility of the proposed method was experimentally verified by using a multi-DOF manipulator. It was confirmed that the MDOB-based decoupling method had better performance than oblique coordinate control. Conventional oblique coordinate control caused oscillation in cases where the modeling error was large and the cutoff frequency of an observer was not high enough to change the system dynamics. On the other hand, the MDOB-based decoupling method became unstable when the difference in mass was large. Zhao *et al.* (2017) proposed an adaptive fuzzy hierarchical sliding-mode control method for a class of multi-input multi-output unknown nonlinear time-delay systems with input saturation. The studied system was first transformed into an equivalent system. Subsequently, based on the sliding-mode control technology and the concept of hierarchical design, a set of adaptive fuzzy hierarchical sliding-mode controllers was designed for the new defined system by using fuzzy systems to approximate uncertain functions and compensate input saturation. Choosing an appropriate Lyapunov–Krasovskii function, it was theoretically proved that all the signals in the closed-loop system together with the proposed sliding surfaces were uniformly ultimately bounded under our designed adaptive fuzzy controllers. Simulation results demonstrated the effectiveness of the proposed design techniques for the systems under consideration. Wang *et al.* (2017) focused on the adaptive control design for a class of high-order Markovian jump nonlinear systems with unmodeled dynamics and unknown dead-zone inputs. By introducing the bound estimation approach, the effects of randomly jumping unknown parameters and the varying dead-zone nonlinearities were tackled. Moreover, aiming at the unmodeled dynamics and completely unknown nonlinear functions, which had Markovian jumping features, several two-layer NNs were introduced for each mode, and the adaptive backstepping control law was established. At last, a numerical example was provided to illustrate the efficiency and advantages of the proposed method. The problem of adaptive tracking control for a class of switched stochastic nonlinear systems in nonstrict-feedback form with unknown nonsymmetric actuator dead-zone and arbitrary switchings was solved by Zhao *et al.* (2015). By combining radial basis function NNs' universal approximation ability and adaptive backstepping technique with common stochastic Lyapunov function method, an adaptive control algorithm was proposed for the considered system. It was shown that the target signal can be almost surely tracked by the system output.

The above decoupling control methods have a large amount of computation, and the algorithm is complex and difficult to realize. The decoupling control about robot is relatively lack, and the researches do not focus on the walking robot, moreover, its control method is difficult to transplant to the walking robot, especially for quadruped robot driven by hydraulic pressure. Because of its high dynamic and high load capacity, the control method is more complex, so it has the practical significance to study the decoupling control among the joints of the hydraulic quadruped robot.

In this paper, according to the cross-coupling problem among the joints of the hydraulic quadruped robot, the coupling model of hip joint and knee joint of hydraulic quadruped robot is established, and the coupling characteristics among joints are studied. On the basis of the multivariable decoupling theory, a reasonable and effective

decoupling control algorithm is proposed to realize the decoupling control among the joints of the hydraulic quadruped robot, which can reduce the coupling effect among the joints of the robot, improve the control precision of the robot, realize the coordinated movement among the joints of the robot and enhance the automation level of the robot.

2. Structure of hydraulic quadruped robot

2.1 Mechanical structure

The framework of the overall structure of the quadruped robot is mainly composed of two parts, the body and legs, and four legs are connected together by the body, which can bear a certain load, and it implements support and walking through the legs, so it is the core part of quadruped robot. To obtain high dynamic, high load capacity and high surface adaptability, a hydraulic cylinder is used as actuator of each joint, and joint type mechanism is adopted for the top configuration. The quadruped robot is driven by hydraulic structure.

The leg structure of quadruped robot has an important influence on the walking ability and the overall flexibility of the robot. Similar to the skeleton of the canine mammal, the legs of the quadruped robot are arranged in a top configuration (Moritz *et al.*, 2016). The single leg of the quadruped robot consists of four joints with a total of four DOFs, of which it has three active DOFs (swing joint, hip joint and knee joint) and one passive DOF (foot). The articulated link mechanism of the joint is adopted in the leg mechanism of the quadruped robot, which has the advantages of simple and compact structure and flexible movement. The connecting rod is made up of body, hip, thigh, calf and ankle, and the joint is composed of swing joint, hip joint, knee joint and foot. The overall mechanism model is shown in Figure 1.

2.2 Driving system

Quadruped robot mainly depends on the four legs of the driving unit to achieve the walking. Quadruped robot is driven by hydraulic drive. Compared to the motor drive, hydraulic drive has large driving torque and rapid response ability, and it can effectively improve the response speed and load capacity of quadruped robot, so the robot can meet the rapid demand under heavy loading. In addition, the hydraulic driving system has high stiffness, high static and dynamic precision and strong anti-interference ability, and the excellent control algorithm is easy to implement, meanwhile, the hydraulic system has the high ratios of power and quality, therefore, hydraulic drive can better simulate the functions of the canine mammal, at the same time, it can provide enough driving torque for the robot in a short period of time, which can increase the load capacity of the robot and meet the need of the robot walking fast (Zhuang *et al.*, 2012).

An asymmetric cylinder is chosen as the hydraulic cylinder of the hydraulic quadruped robot, which has the advantages of simple structure, large bearing capacity, and can meet the requirements of the robot to walk fast under heavy load. To improve the control accuracy and response speed, the flow valve of the high performance and small size is selected as the servo valve. The hydraulic system of the quadruped robot adopts the method of constant pressure variable oils supply, so as to improve the efficiency of the hydraulic system and reduce the volume and weight of the hydraulic system. The schematic diagram of the hydraulic system is shown in Figure 2.

In Figure 2, 1 is the fuel tank, 2 and 11 are oil filter, 3 is the servo valve, 4 is a hydraulic cylinder, 5 represents a constant pressure variable pump, 6 is the throttle valve, 7 is cooler, 8 is a one-way valve, 9 is unloading valve, 10 is the relief valve, 12 is a gauge, 13 is the pressure sensor and 14 is the accumulator.

Each leg has three active DOFs, and it is composed of three double acting single rod hydraulic cylinders. The movements of the hydraulic cylinders are controlled by three electro-hydraulic servo valves. The hydraulic pump is an axial piston pump, and the oil filter is installed at the inlet to prevent the damage to the hydraulic pump. To prevent the backflow of hydraulic oil, a one-way valve is arranged between the oil filter and the hydraulic pump. When the system pressure exceeds the limit value, the relief valve plays a major role in safety. The oil filter is connected to the oil return path to absorb impurities. Accumulator is used as emergency fuel supply. The cooler uses an air-cooled form. Pressure gauge shows the pressure state when the system is working. The key parameters of the hydraulic system are shown in Table I.

3. Mathematical model for leg of hydraulic quadruped robot

On the basis of establishing rules of robot D-H coordinate system, the D-H coordinate system for leg of the hydraulic driven quadruped robot is built, because the leg of the

Figure 1 Overall framework of hydraulic quadruped robot

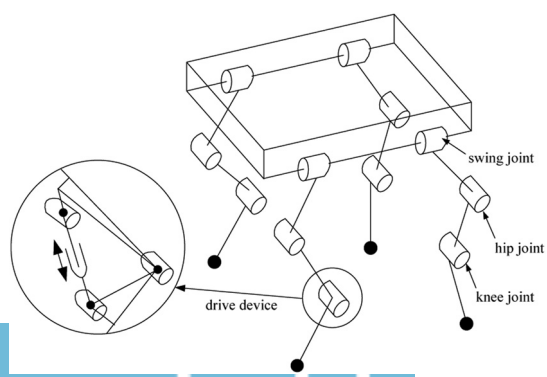

Figure 2 Principle diagram of the hydraulic system

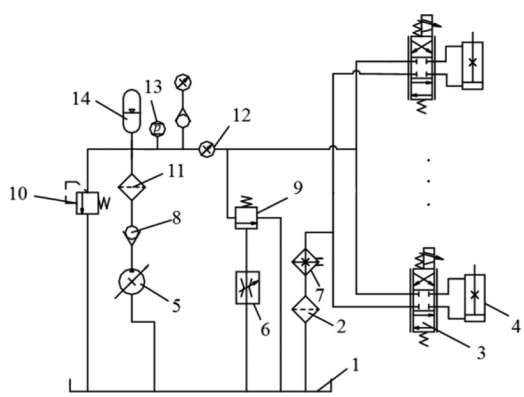

Table I Key parameters of the hydraulic system

Hydraulic system parameters	Corresponding value
System pressure (MPa)	24
Inner diameter of hydraulic cylinder (mm)	28
Piston rod diameter (mm)	16
Piston rod stroke (mm)	70
Rated flow of servo valve (L/min)	11.5 ± 0.8
Servo valve flow gain ((L/min)/mA)	0.77 ± 0.055

hydraulic quadruped robot uses the top configuration structure, so the robot's four legs have exactly the same D-H coordinates (Ding *et al.*, 2012), and the D-H coordinate system of one leg is shown in Figure 3.

As shown in Figure 3, the length of the bar AB is defined as l_1, the length of the bar BC is defined as l_2, the length of the bar CD is defined as l_3; the rotation angle of the swing joint is θ_1, the rotation angle of the hip joint is θ_2, the rotation angle of the knee joint is θ_3; the quality of AB, BC, CD is m_1, m_2, m_3, respectively; the generalized coordinates of the leg are defined as $q = [\theta_1, \theta_2, \theta_3]^T$. The robot's D-H coordinate system is established, and the parameters of the connecting rods of the single leg are shown in Table II.

3.1 Dynamics model of the leg

The dynamic model of leg system is established by the Lagrange method. As this paper studies the coupling between the thigh and calf, it only needs to establish the dynamic model of the thigh and calf. It can be seen from Figure 3, the thigh and calf of the robot swing in the XOZ plane, the kinetic energy of

Figure 3 D-H coordinate of one leg of hydraulic quadruped robot

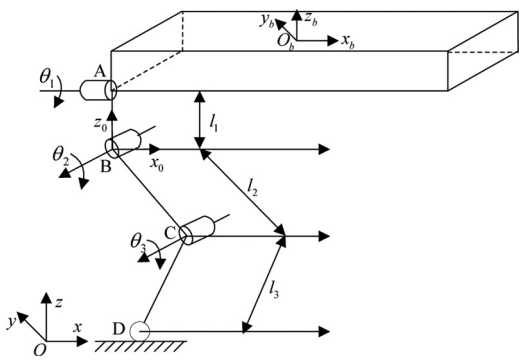

Table II D-H parameters of single leg

Connecting rod i	Length of connecting rod L_{i-1}	Twist angle of joint α_{i-1}°	Distance of joint d_i	Rotation angle of joint θ_i
1	0	0°	0	θ_1
2	L_1	90°	0	θ_2
3	L_2	0°	0	θ_3
4	L_3	0°	0	0°

the rod BC is set to E_{K2}, and the potential energy is E_{P2}. Because $v_2 = l_2\dot{\theta}_2$, $E_{K2} = 1/2m_2{v_2}^2$, $h_2 = l_1 + l_2\cos\theta_2$ and $E_{P2} = m_2gh_2$, the kinetic energy and potential energy of the thigh BC are:

$$E_{K2} = \frac{1}{2}m_2{l_2}^2{\dot{\theta}_2}^2 \tag{1}$$

$$E_{P2} = m_2g(l_1 + l_2\cos\theta_2) \tag{2}$$

Similarly, the kinetic energy of the calf CD is:

$$E_{K3} = \frac{1}{2}m_3\left[{l_2}^2{\dot{\theta}_2}^2 + {l_3}^2(\dot{\theta}_2 + \dot{\theta}_3)^2 + 2l_2l_3\dot{\theta}_2(\dot{\theta}_2 + \dot{\theta}_3)\cos\theta_3\right] \tag{3}$$

The potential energy of the calf CD is:

$$E_{P3} = m_3g(l_1 + l_2\cos\theta_2 + l_3\cos(\theta_2 + \theta_3)) \tag{4}$$

For the mechanical system of the quadruped robot, its Lagrange function is:

$$\begin{aligned} L &= E_K + E_P = (E_{K2} + E_{K3}) + (E_{P2} + E_{P3}) \\ &= \frac{1}{2}m_2{l_2}^2{\dot{\theta}_2}^2 + \frac{1}{2}m_3\left[{l_2}^2{\dot{\theta}_2}^2 + {l_3}^2(\dot{\theta}_2 + \dot{\theta}_3)^2\right] \\ &\quad + m_3l_2l_3\dot{\theta}_2(\dot{\theta}_2 + \dot{\theta}_3)\cos\theta_3 + m_2g(l_1 + l_2\cos\theta_2) \\ &\quad + m_3g[l_1 + l_2\cos\theta_2 + l_3\cos(\theta_2 + \theta_3)] \end{aligned} \tag{5}$$

To get the dynamic equation of the system, Lagrange equation (5) is differentiated to obtain the torques of the joints:

$$\frac{d}{dt}\frac{\partial L}{\partial\dot{\theta}_i} - \frac{\partial L}{\partial\theta_i} = \tau_i \qquad i = 2, 3 \tag{6}$$

The standard form of the kinetic model is written as follows:

$$\begin{bmatrix}\tau_2\\ \tau_3\end{bmatrix} = M(\theta)\begin{bmatrix}\ddot{\theta}_2\\ \ddot{\theta}_3\end{bmatrix} + C(\theta,\dot{\theta})\begin{bmatrix}\dot{\theta}_2\\ \dot{\theta}_3\end{bmatrix} + G(\theta) \tag{7}$$

By calculating:

$$M(\theta) = \begin{bmatrix} m_2{l_2}^2 + m_3({l_2}^2 + {l_3}^2 + 2l_2l_3\cos\theta_3) & m_3{l_3}^2 + m_3l_2l_3\cos\theta_3 \\ m_3{l_3}^2 + m_3l_2l_3\cos\theta_3 & m_3{l_3}^2 \end{bmatrix} \tag{8}$$

$$C(\theta,\dot{\theta}) = \begin{bmatrix} -m_3l_2l_3\sin\theta_3\dot{\theta}_3 & -m_3l_2l_3\sin\theta_3(\dot{\theta}_2 + \dot{\theta}_3) \\ m_3l_2l_3\sin\theta_3\dot{\theta}_2 & 0 \end{bmatrix} \tag{9}$$

$$G(\theta) = \begin{bmatrix} m_2gl_2\sin\theta_2 + m_3gl_2\sin\theta_2 + m_3gl_3\sin(\theta_2 + \theta_3) \\ m_3gl_3\cos(\theta_2 + \theta_3) \end{bmatrix} \tag{10}$$

To facilitate the presentation, the equation is simplified as follows:

$$T = M(q)\ddot{q} + C(q,\dot{q})\dot{q} + G(q) \tag{11}$$

In the equation, $q = [\theta_1, \theta_2, \theta_3]^T$, $M(q)$ is inertia matrix, $C(q,\dot{q})$ is concentric acceleration and $G(q)$ is gravity term.

Because the driving force of the dynamic model is the torque, and the actual output of the hydraulic cylinder is force, it is necessary to transform the force and torque. In the case of the hip joint, the conversion between the force and the torque is shown in Figure 4.

The output force of the hydraulic cylinder F_2 is decomposed into F_{21} along the AF direction, and F_{22} perpendicular to the AF direction. The torque T_2 is generated by force F_{22}, after calculation:

$$T_2 = \frac{l_{AF} \cdot l_{AE} \sin\left(\beta - \frac{\pi}{4}\right)}{\sqrt{l^2_{AF} + l^2_{AE} - 2l_{AF} \cdot l_{AE} \cos\left(\beta - \frac{\pi}{4}\right)}} F_2 \tag{12}$$

For this reason, the relationship between the output force of the cylinder and the generalized driving torque can be described as follows:

$$T = \mathcal{J}_0 F \tag{13}$$

In the equation, $F = [F_1, F_2, F_3]^T$, the output force of the three hydraulic cylinders is F_1, F_2, F_3.

In fact, the matrix $\mathcal{J}_0$ is the Jacobi matrix of the corresponding length of each cylinder, which is similar to the relationship between the driving force and the driving torque. The relationship between the displacement of the cylinder and the joint angle can be obtained as follows:

$$y = \mathcal{J}_0 q \tag{14}$$

In the equation, $y_i (i = 1, 2, 3)$ is displacement of each hydraulic cylinder.

Therefore, we can transform equation (11) to obtain the dynamic model between the displacement and the output force of the hydraulic cylinder:

$$\mathcal{J}_0 F = M(q)\mathcal{J}_0^{-1}\ddot{y} + C(q,\dot{q})\mathcal{J}_0^{-1}\dot{y} + G(q) \tag{15}$$

After finishing, the above equation can be abbreviated as:

$$F = M(y)\ddot{y} + C(y,\dot{y})\dot{y} + G(y) \tag{16}$$

wherein, $M(y) = (\mathcal{J}_0^{-1})^2 M(q)$, $C(y,\dot{y}) = \left(\mathcal{J}_0^{-1}\right)^2 C(q,\dot{q})$, $G(y) = \mathcal{J}_0^{-1} G(q)$.

Figure 4 Relation between driven torque and output force of hydraulic cylinder

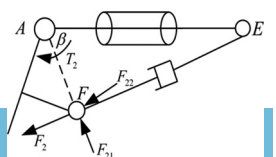

3.2 Model of hydraulic servo-driven system

For general motion control, driven system model is often neglected, if only considering the dynamics model, we usually think that the output of the driven system (the input of dynamic model) and the control rules are proportional. However, in the process of the robot control, the robot's motion is controlled by the input voltage of the servo valve. Therefore, the driving torque and the input voltage of the servo valve cannot be simply considered as proportional relationship, or a simple first-order or two-order differential equation. Therefore, to design the motion control law, which is in accordance with the actual situation, it is necessary to carry on the modeling and analysis of the hydraulic servo-driven system of the robot.

According to the maximum flow of the different hydraulic cylinders at the same time, the hydraulic pump is designed, and the accumulator can supply emergency, so, in the normal condition, if the amount of leakage of hydraulic oil is few, it may be considered that the flow of the hydraulic cylinder is independent of each other.

Before the analysis, we first assumed that the return oil pressure is zero, the supply oil pressure is constant and the elastic modulus and temperature of oil can be considered as constant. The types and the parameters of the hydraulic cylinder and servo valve are the same for the joints of robot, therefore, we only analyze one of those, the rest are similar.

First of all, the servo valve is analyzed, the working mode is to adjust the spool displacement x_v by the size and direction of the servo valve input voltage U_1, when U_1 is right, $x_v > 0$, the piston rod moves in the right direction; when U_1 is negative, $x_v < 0$, the piston rod moves along the negative direction. The pressure-flow equation of the servo valve is deduced:

$$Q_L = c_d \omega x_v \sqrt{\frac{1}{\rho}\left(P_s - \frac{x_v}{|x_v|} P_L\right)} \tag{17}$$

Among them, P_s is the supply pressure, ω is area gradient of orifice, c_d is servo valve orifice flow coefficient and ρ is the density of the hydraulic oil.

From the performance manual of the servo valve, it can be seen that x_v and U_1 are proportional, then:

$$Q_L = k' U_1 \sqrt{\frac{1}{\rho}\left(P_s - \frac{U_1}{|U_1|} P_L\right)} \tag{18}$$

wherein, $k' = c_d \omega$.

The hydraulic cylinder is quantitatively analyzed. When the system is in steady state, the hydraulic cylinder satisfies the force balance equation and the flow continuity equation:

$$p_1 A_1 - p_2 A_2 = F_1 \tag{19}$$

$$\frac{Q_1}{A_1} = \frac{Q_2}{A_2} \tag{20}$$

In the equation, p_1 and p_2 represent the pressure of the left and right cavities, A_1 and A_2 represent the effective area of the left and right cavities and Q_1 and Q_2 represent the flow of the left and right cavities.

The load flow is defined as:

$$Q_{L1} = \frac{Q_1 + nQ_2}{1 + n^2} \tag{21}$$

$n = A_2/A_1$ is the ratio of the effective area of the two cavity.

When the movement speed of the piston is greater than 0, the input voltage of the servo valve is positive, and the load flow is derived using equations (18)-(21):

$$Q_{L1} = kU_1\sqrt{p_s - p_{L1}} \tag{22}$$

where in, $k = k'\sqrt{\frac{2}{1+n^3}}$.

Because the legs of the hydraulic quadruped robot are positioned at the initial position, the piston rod of each hydraulic cylinder is in the middle position. Therefore, the combined equations (21) and (22) can be obtained:

$$kU_1\sqrt{p_s - p_{L1}} = A_1\frac{dy_1}{dt} + \frac{V_t}{2(1+n^2)\beta_e}\frac{dp_{L1}}{dt} + C_{tc1}p_{L1} \tag{23}$$

In the formula, V_t is an effective volume of hydraulic cylinder, β_e is elastic modulus of hydraulic oil and C_{tc1} is related to the internal leakage parameters of the hydraulic cylinder C_{tc}, $C_{tc1} = \frac{1+n}{(1+n^3)}C_{tc}$.

Hydraulic quadruped robot can complete the walking movement, and it mainly depends on the output force in the direction of elongation of the hydraulic cylinder, so the forward motion of the piston rod is considered, and the corresponding situation is shown in equation (23).

Both sides of equation (23) are multiplied by A_1 at the same time:

$$\frac{2k(1+n^2)\beta_e A_1}{V_t}\sqrt{p_s - p_{L1}}U_1 = \dot{F}_1 + \frac{2(1+n^2)\beta_e C_{tc1}}{V_t}F_1 + \frac{2(1+n^2)\beta_e {A_1}^2}{V_t}\dot{y}_1 \tag{24}$$

The three hydraulic cylinders of the single leg have the same type and parameters, so the model for the whole hydraulic servo-driven system of the single leg can be simplified:

$$k_0 \mathfrak{J} U = \dot{F} + BF + E\dot{y} \tag{25}$$

3.3 Coupling model of hip joint and knee joint

The walking of the hydraulic quadruped robot is mainly dependent on the two active degrees of freedom of the hip joint and knee joint. Only when the robot slips or turns, the hydraulic cylinder of the swing joint starts to move. Then, when the robot is in the direction of walking, the hip is not moving, only the hip joint and knee joint rotate, and drive the movement of the foot, therefore, this paper only considers the coupling between the thigh and the calf, so the coupling between the hip joint and the knee joint is considered.

In the process of movement, the joint motion of the hydraulic quadruped robot is low speed, and the coriolis force and the centripetal force have little effect on the movement of the joint, so they are negligible, but it is affected by the inertia force and gravity, to facilitate the analysis. It only considers the effect of inertia force and gravity, and the coriolis force and the centripetal force are ignored (Chi *et al.*, 2001), so that the dynamic model of leg of the hydraulic quadruped robot is changed into the following form:

$$F = M(y)\ddot{y} + G(y) \tag{26}$$

Thus, the dynamic relationships between the output of the hip joint and the knee joint and the displacement of the hydraulic cylinder are as follows:

$$\begin{cases} F_2 = M_{21}\ddot{y}_2 + M_{22}\ddot{y}_3 + G_{21}y_2 + G_{22}y_3 \\ F_3 = M_{31}\ddot{y}_2 + M_{32}\ddot{y}_3 + G_{31}y_2 + G_{32}y_3 \end{cases} \tag{27}$$

wherein, $\begin{bmatrix} M_{21} & M_{22} \\ M_{31} & M_{32} \end{bmatrix}$ is the inertia matrix, and $\begin{bmatrix} G_{21} & G_{22} \\ G_{31} & G_{32} \end{bmatrix}$ is the gravity term.

The Laplace transform of equation (27) can be obtained as follows:

$$\begin{cases} y_2(s) = \dfrac{F_2 - G_{22}y_3(s) - M_{22}s^2y_3(s)}{M_{21}s^2 + G_{21}} \\ y_3(s) = \dfrac{F_3 - G_{31}y_2(s) - M_{31}s^2y_2(s)}{M_{32}s^2 + G_{32}} \end{cases} \tag{28}$$

It can be seen from equation (28) that the output of the hip joint y_2 affects the output of the knee joint y_3, and the output of the knee joint y_3 also affects the output of hip joint y_2, so there is obvious coupling between the thigh and the calf of the hydraulic quadruped robot.

4. Design neural network model reference decoupling controller

The structure of the NN model reference decoupling controller is the same as the model reference adaptive controller, and it just uses the NN instead of the controller and identifier in the system. Then the neural network controller (NNC) and neural network identifier (NNI) are constructed (Tahoun, 2012; Engeberg, 2013), and the structure of the NN model reference decoupling control is shown in Figure 5.

On the basis of the control requirements of the controlled object, a reference model is designed to meet the performance of the controlled object. The outputs of the reference model specify the desired performance indexes; however, when the parameters of the controlled object change or are affected by the external disturbances, the output $y(t)$ of the system and the output $y_o(t)$ of the ideal reference model will not be consistent, and the two outputs are compared to get the deviation signal $e_2(t)$. When the signal $e_2(t)$ enters the NN controller, after the learning and training of the NN controller, the parameters of the controller and the decoupling network are adjusted adaptively. The output $y(t)$ of the controlled object is changed

Figure 5 Structure of the neural network model reference decoupling controller

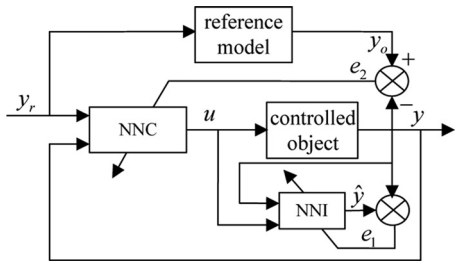

to match the output $y_o(t)$ of the reference model until the deviation signal $e_2(t)$ approaches zero. At the same time, the NN identifier is trained off-line, which can be used to predict the next output of the system according to the current and previous input and output of the controlled object. In this way, the variable parameter control and decoupling control are realized by NN model reference decoupling network.

4.1 Establish reference model

The first step of the NN model reference decoupling control is to set the reference model of the system without coupling. The dynamic model of equation (28) is brought into the hydraulic system model of equation (25), and the model of the whole control system can be obtained as follows:

$$k_0\mathcal{J}\begin{bmatrix}u_2(s)\\u_3(s)\end{bmatrix} = \begin{bmatrix}M_{21}s^3 + BM_{21}s^2 + (G_{21}+E)s + BG_{21} & (1+B)M_{22}s^2 + (1+B)G_{22}\\(1+B)M_{31}s^2 + (1+B)G_{31} & M_{32}s^3 + BM_{32}s^2 + (G_{32}+E)s + BG_{32}\end{bmatrix}\begin{bmatrix}y_2(s)\\y_3(s)\end{bmatrix} \tag{29}$$

In equation (29), the product of the main diagonal element represents the transfer function of the joint between the thigh and the calf, and the non-diagonal term is the coupling term between the thigh joint and the calf joint.

Formula (29) is the coupling model between the thigh and the calf of the hydraulic quadruped robot. If the coupling term of the secondary diagonal in equation (29) is removed, the reference model between the thigh and the calf without coupling can be obtained as follows:

$$\begin{cases} y_2(s) = \dfrac{k_0\mathcal{J}}{M_{21}s^3 + BM_{21}s^2 + (G_{21}+E)s + BG_{21}}u_2(s) \\ y_3(s) = \dfrac{k_0\mathcal{J}}{M_{32}s^3 + BM_{32}s^2 + (G_{32}+E)s + BG_{32}}u_3(s) \end{cases} \tag{30}$$

4.2 Design neural network identifier

Because the single leg of the hydraulic quadruped robot has only two joints in the forward direction, in the hip fixed conditions, the single leg system of the robot is a multivariable system with two inputs and two outputs; therefore, the structure of NN identifier is also two inputs and two outputs as shown in Figure 6.

Figure 6 Neural network identifier

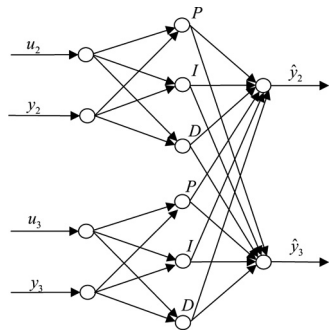

In Figure 6, u_2 and u_3 are the input of the controlled object, y_2 and y_3 are the output of the controlled object and $\hat{y}_2$ and $\hat{y}_3$ are the output of the forecast.

The NN identifier is based on the current and previous input and output of the controlled object to predict the next output $\hat{y}(k+1)$ of the system, thus, the error between predicted output and the actual output of the system can be obtained as:

$$e_1(k+1) = \hat{y}(k+1) - y(k+1) \tag{31}$$

Using $e_1(k+1)$ to adjust the weights of the NN identifier, the objective function of the NN identifier is:

$$\mathcal{J}_1 = \sum_{i=0}^{T_1}\|e_1(k+1)\|^2 \tag{32}$$

wherein, T_1 is the identification cycle.

4.3 Design neural network controller

Same as the NN identifier, the structure of the NN controller is also two inputs and two outputs, and the structure is shown in Figure 7.

y_{r2} and y_{r3} are the given input signals, y_2 and y_3 are the output of the controlled object and u_2 and u_3 are the control variable of the system.

The error between the output of the reference model and the actual output of the system is:

$$e_2(k) = y(k) - y_o(k) \tag{33}$$

The NN controller adjusts the $u(k)$ according to the error $e_2(k)$, so that the controlled object can track the output of the reference model:

$$\mathcal{J}_2 = \sum_{i=0}^{T_2}\|e_2(k+1)\|^2 = \sum_{i=0}^{T_2}\|y(k) - y_o(k)\|^2 \tag{34}$$

wherein, T_2 is the identification cycle.

In general, it is difficult to correct the weight of the NN controller by the actual output $y(k)$ of the controlled object, and the output $\hat{y}(k)$ predicted by the NN identifier can be used in place of the actual output $y(k)$ of the controlled object. Thus, the objective function of the improved NN controller can be approximated as:

Figure 7 Neural network controller

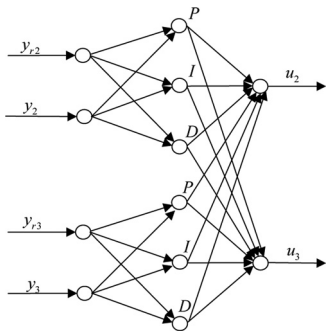

$$\mathcal{J}_2 \approx \sum_{i=0}^{T_2} \|\hat{y}(k) - y_o(k)\|^2 \tag{35}$$

5. Simulation analysis

To verify the effectiveness of the proposed decoupling control algorithm, the control loop of the NN model reference decoupling control algorithm is built in MATLAB/Simulink to detect the decoupling effect. In the previous section, the coupling model of the dynamic mechanisms between hip joint and knee joint of hydraulic quadruped robot has been derived. The proposed decoupling control algorithm is applied to the leg system of the robot to verify its decoupling effectiveness on the hip joint and knee joint of the hydraulic quadruped robot.

5.1 Simulation of the coupling effect from hip joint to knee joint

To be convenient, the given signal is a step signal, for the coupling effect from the hip joint to the knee joint, the input of the hip joint is the step signal with the initial value of 35 mm and the amplitude of 15 mm, and the input of the knee joint is a constant value of 35 mm. The simulations are carried out under PID decoupling method and the NN model reference decoupling control algorithm, and the parameters of PID decoupling controller are obtained by the cut-and-trial method. The corresponding response curves are shown in Figure 8 and Figure 9.

In Figures 8 and 9, Curve 1 is the ideal output curve of the hip joint, Curve 2 is the response curve of the hip joint, Curve 3 is the ideal output curve of the knee joint and Curve 4 is the coupling response curve of the knee joint.

5.2 Simulation of the coupling effect from knee joint to hip joint

For the coupling effect from the knee joint to the hip joint, the input of the knee joint is the step signal with the initial value of 35 mm and the amplitude of 15 mm, and the input of the hip joint is a constant signal of 35 mm. The simulations are carried out under the PID decoupling method and the NN model reference decoupling control algorithm, and the parameters of PID decoupling controller are obtained by the cut-and-trial method. The corresponding response curves are shown in Figures 10 and 11.

Figure 8 Simulation curves with PID decoupling control

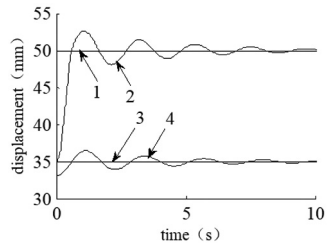

Figure 9 Simulation curves with neural network model reference decoupling control

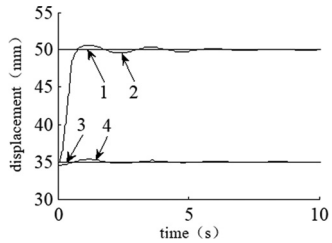

Figure 10 Simulation curves with PID decoupling control

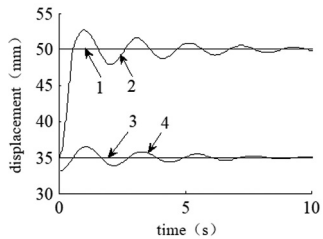

In Figures 10 and 11, Curve 1 is the ideal output curve of the knee joint, Curve 2 is the response curve of the knee joint, Curve 3 is the ideal output curve of the hip joint and Curve 4 is the coupling response curve of the hip joint.

5.3 Simulation results analysis

According to the simulation results shown in Figures 8 and 11, there is a coupling relationship between the hip joint and the knee joint of the single leg, and the coupling effect from hip joint to knee joint is similar to that from knee joint to hip joint.

Figure 11 Simulation curves with neural network model reference decoupling control

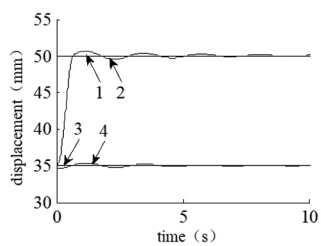

Taking the coupling effect from hip joint to knee joint as an example, using the PID decoupling measures, the maximum overshoot of the response curve of hip joint reaches about 16.8 per cent, the output fluctuation is about five times before it is stable, the maximum error of the coupling curve of the knee joint is about 3.12 mm and the coupling effect from knee joint to hip joint is about 8.9 per cent, so there is a big coupling between two joints. In the same given signals, using the NN model reference decoupling control method, the maximum overshoot of the response curve of the hip joint reaches about 4.15 per cent, output fluctuation is about two times, the maximum error of knee joint coupling curve is about 0.73 mm and the coupling effect from hip joint to knee joint is about 2.1 per cent, which can better reduce the coupling.

6. Experimental verification

The mechanical structure of the single leg is shown in Figure 12. The hip and knee joints are driven by an electro-hydraulic servo actuator, and the foot is mounted with linear bearing and spring to damp vibration and store energy. The material of leg selects super-hard alloy, both to reduce their own weight, but also to ensure strength. The foot is wrapped by the rubber, which can play the role of absorption vibration and anti-skid.

The structure parameters of the leg are shown in Table III.

The measurement and control systems are used to complete the test and control the robot, and the equipments used in experiment are shown in Table IV. The control signals are transformed and amplified to electro-hydraulic servo valve to control the movement of the hydraulic cylinder through the data acquisition card and servo valve amplifier. The feedback signals from the sensors are transmitted to the industrial personal computer through the conditioning circuit and data acquisition card to achieve the control of the electro-hydraulic servo system.

6.1 Experiment of the coupling effect from hip joint to knee joint

To verify the coupling effect from the hip joint to the knee joint, the input of the hip joint is a sine signal with the frequency of 1Hz, and the amplitude is 7.5 mm, the offset is 35 mm and the input of the knee joint is a constant value of 35 mm. The experimental studies are carried out under the PID decoupling measure and the NN model reference decoupling control algorithm, and the second-order active low-pass filters are used in experiment to process the feedback signals. The experimental results are shown in Figures 13 and 14.

In Figures 13 and 14, Curve 1 is the ideal output of the hip joint, Curve 2 is the actual output of the hip joint, Curve 3 is the ideal output of the knee joint and Curve 4 is the coupling response of knee joint.

6.2 Experiment of the coupling effect from knee joint to hip joint

For the coupling effect from the knee joint to the hip joint, the input of the knee joint is a sine signal with the frequency of 1 Hz, and the amplitude is 7.5 mm and the offset is 35 mm, and the input of the hip joint is a constant value of 35 mm. The experimental studies are carried out under the PID decoupling measure and the NN model reference decoupling control algorithm, and the second-order active low-pass filters are used in experiment to process the feedback signals. The experimental results are shown in Figures 15 and 16.

Table III Structure parameters of the leg

Structure parameters of the leg	Value
Weight of the single leg (kg)	12.10
Weight of hip (kg)	2.72
Weight of thigh (kg)	3.59
Weight of calf (kg)	1.59
Weight of foot (kg)	0.95
Initial height of the body (m)	0.650
Length of thigh (m)	0.340
Length of calf (m)	0.330
Initial distance of the knee joint and foot (m)	0.330
Spring stiffness (N/m)	20,000
Spring damping (N/m/s)	300

Table IV Equipments of the measurement and control

Equipment	Type
Data acquisition card	PCI-1716HG
Asymmetric servo valve	SFL212F-12/8-21-40
Servo amplifier	OPA57, OPA27
Displacement sensor	LVDT-PA1HL60X

Figure 12 Structure of the single leg of hydraulic quadruped robot

Figure 13 Experiment curves with PID decoupling control

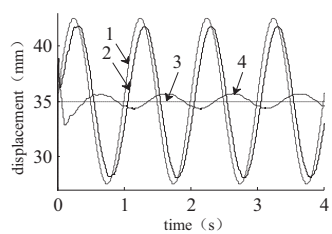

Figure 14 Experiment curves with neural network model reference decoupling control

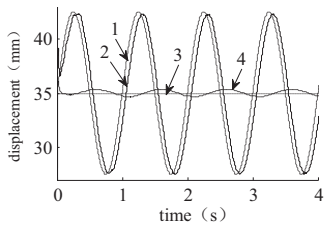

In Figures 15 and 16, Curve 1 is the ideal output of the knee joint, Curve 2 is the actual output of the knee joint, Curve 3 is the ideal output of the hip joint and Curve 4 is the coupling response of hip joint.

6.3 Experimental results analysis

The experimental results of Figures 13 and 16 show that the coupling effect from hip joint to knee joint is similar to that from knee joint to hip joint. Taking the coupling effect from hip joint to knee joint as an example to analyze the actual decoupling effect, using the PID decoupling measure, the phase lag of the response curve of the hip joint is about 19.7 degrees, the amplitude attenuation is about 1.61 per cent, the maximum error of the coupling curve of the knee joint is about 0.61 mm and the coupling effect from knee joint to hip joint is about 1.4 per cent, so there is a big coupling between two joints. Using the NN model reference decoupling control method, the phase lag of the response curve of the hip joint is about 16.4 degrees, the amplitude attenuation is about 0.51 per cent, the maximum error of the coupling curve of the knee joint is about 0.31 mm and the coupling effect from knee joint to hip joint is about 0.91 per cent, which can better achieve the decoupling.

Figure 15 Experiment curves with PID decoupling control

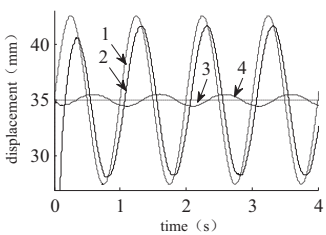

Figure 16 Experiment curves with neural network model reference decoupling control

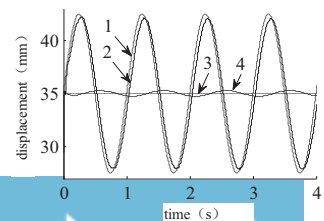

The results of the experiment and simulation are basically consistent, which shows that the proposed NN model reference decoupling control method can reduce the cross-coupling between the hip joint and knee joint, reaching the purpose of decoupling for each joint of the robot.

7. Conclusion

Aiming at the problem of cross-coupling for the leg of the hydraulic quadruped robot, the dynamics equations of the leg are derived; furthermore, the coupling dynamics relationships between the thigh and the calf of quadruped robot are obtained, and expound the necessity of decoupling control. An NN model reference decoupling controller is designed on the basis of the multivariable decoupling theory. Finally, the simulation and experiment are carried out between the thigh joint and the calf joint of the hydraulic quadruped robot, and the results show that the proposed NN model reference decoupling control method is effective, and this method can reduce the cross-coupling between the thigh and the calf and improve the dynamic characteristics of the single joint of the leg. This paper has studied the coupling characteristics and decoupling methods among the different joints for the leg of hydraulic robot, in the actual movement of the robot, there is not only the coupling among joints of the leg but also a certain coupling relationship among the four legs of the robot; therefore, how to achieve the decoupling among the four legs of the robot is the research direction in the future.

References

Chi, R.N., Hu, Y.M. and Hu, Z.X. (2001), "Real-time trajectory tracking of nonholonomic mobile robot based on decoupling control techniques", *Robot*, Vol. 23 No. 3, pp. 256-260.

Ding, Y.S. and Liu, B. (2011), "An intelligent bi-cooperative decoupling control approach based on modulation mechanism of internal environment in body", *IEEE Transactions on Control Systems Technology*, Vol. 19 No. 3, pp. 692-698.

Ding, Y.S., Liu, B. and Ren, L.H. (2007), "Intelligent decoupling control system inspired from modulation of the growth hormone in neuroendocrine system", *Dynamics of Continuous Discrete and Impulsive Systems-Series B-Applications & Algorithms*, Vol. 14 No. 5, pp. 679-693.

Ding, L.H., Wang, R.X., Feng, H.S. and Li, J. (2012), "Brief analysis of a BigDog quadruped robot", *Chinese Journal of Construction Machinery*, Vol. 23 No. 5, pp. 505-514.

Engeberg, E.D. (2013), "Human model reference adaptive control of a prosthetic hand", *Journal of Intelligent and Robotic Systems: Theory and Applications* , Vol. 72 No. 1, pp. 41-56.

Iván, G.H., Xavier, K., Julien, G., Coleman, R.C. and Barre, P.J. (2012), "Model-based decoupling control method for dual-drive gantry stages: a case study with experimental validations", *Control Engineering Practice*, Vol. 6 No. 15, pp. 12-16.

Kayacan, E., Zeki, Y.B. and Saeys, W. (2011), "Modeling and control of a spherical rolling robot: a decoupled dynamics approach", *Robotica*, Vol. 30 No. 4, pp. 671-680.

Lin, H.N. and Kuroe, Y. (1995), "Decoupling control of robot manipulators by using variable-structure disturbance observer", *IECON Proceedings*, Vol. 2, pp. 1266-1271.

Liu, Y.B., Han, X.Y. and Zhao, X.H. (2009), "Decoupled control of a 3-RRRT parallel robot", *Journal of Harbin Institute of Technology*, Vol. 12 No. 41, pp. 247-249.

Luo, S.W., Wu, Z.S. and Zhang, Q. (1992), "Research on optimum decoupling control of electro – hydraulic servo system for joint type robot", *Machine Tool & Hydraulics*, No. 5, pp. 224-228.

Michael, R. and Makoto, I. (2015), "Control of nonlinear elastic joint robots using feed-forward torque decoupling", *IFAC*, Vol. 48 No. 11, pp. 137-142.

Moritz, M., André, O. and Konstantin, K. (2016), "Robot-assisted landing of VTOL UAVs: design and comparison of coupled and decoupling linear state-space control approaches", *IEEE Robotics and Automation*, Vol. 1 No. 1, pp. 114-121.

Nicuols, N.K. (1982), "Time-optimal decoupling control problems", *International Journal of Control*, Vol. 35 No. 5, pp. 453-456.

Nikolaou, M. and Hanagandi, V. (1995), "Recurrent neural networks in decoupling control of multivariable nonlinear systems", *Chemical Engineering Communications*, Vol. 136 No. 1, pp. 211-219.

Tahoun, A.H. (2012), "Model reference adaptive control of unknown unified chaotic systems", *Mediterranean Journal of Measurement and Control*, Vol. 8 No. 2, pp. 408-412.

Takahiro, N., Takahiro, M. and Kouhei, O. (2014), "Decoupling strategy for position and force control based on modal space disturbance observer", *IEEE Transactions on Industrial Electronics*, Vol. 61 No. 2, pp. 1022-1032.

Wang, H.R., Fang, Y.M., Jiao, X.H. and Song, W.G. (1994), "Design robust decoupling controller based on state feedback", *Control and Decision*, Vol. 4 No. 9, pp. 306-310.

Wang, Z., Yuan, J.P., Pan, Y.P. and Che, D.J. (2017), "Adaptive neural control for high order Markovian jump nonlinear systems with unmodeled dynamics and dead zone inputs", *Neurocomputing*, Vol. 247, pp. 62-72.

Zhao, X.D., Shi, P., Zheng, X.L. and Zhang, L.X. (2015), "Adaptive tracking control for switched stochastic nonlinear systems with unknown actuator dead-zone", Vol. 60, pp. 193-200.

Zhao, X.D., Yang, H.J., Xia, W.G. and Wang, X.Y. (2017), "Adaptive fuzzy hierarchical sliding-mode control for a class of MIMO nonlinear time-delay systems with input saturation", *IEEE Transactions on Fuzzy Systems*, Vol. 25 No. 5, pp. 1062-1077.

Zhuang, M., Yu, Z.W., Gong, D.P., Xu, M.L. and Dai, Z.D. (2012), "Gait planning and simulation of quadruped robot with hydraulic drive based on ADAMS", *Machinery Design & Manufacture*, No. 7, pp. 100-102.

Corresponding author

Bingwei Gao can be contacted at: gaobingwei_happy@163.com